Phonon Raman scattering in $InSb/In_{1-x}Al_xSb$ strained-layer superlattices

V. P. Gnezdilov,* D. J. Lockwood, and J. B. Webb

Institute for Microstructural Sciences, National Research Council, Ottawa, Ontario, Canada K1A 0R6

(Received 22 December 1992)

Raman scattering has been used to study a variety of $InSb/In_{1-x}Al_xSb$ strained-layer superlattices grown by magnetron sputter epitaxy. The observed frequencies of zone-folded longitudinal acoustic phonons agree well with those calculated using Rytov's theory of acoustic vibrations in layered media. The intensities of these phonons do not coincide with those calculated within the regime of the photo-elastic mechanism for light scattering because the exciting light energy is close to resonance with super-lattice electronic transitions. The longitudinal optic phonons in $In_{1-x}Al_xSb$ layers exhibit two-mode behavior and their shift due to the intralayer strain is discussed.

I. INTRODUCTION

Semiconductor superlattices have now been of interest for nearly 20 years. Such interest has been stimulated through potential device applications of superlattices, because of their unusual transport and optical properties, and by the development of new growth techniques capable of stable and reproducible growth of crystals composed of alternating layers of two semiconductors. Raman spectroscopy has been one of the most widely employed experimental tools in the study of superlattices and in the characterization of the materials used in devices.[1,2] In particular, Raman scattering allows one to obtain, for example, information on the vibrational properties, on the crystalline quality, on the strain within the superlattice layers, and on special kinds of ordering within the alloy layers.

In this paper, we report the results of a light scattering study of the acoustic and optic phonons in $InSb/In_{1-x}Al_xSb$ strained-layer superlattices grown by magnetron sputter epitaxy[3] (MSE) with different aluminum concentrations in the range $0 < x < 0.5$. This system is particularly interesting since information regarding InSb-based alloys is very limited and the high electron mobility and small effective mass associated with InSb would suggest superior performance of devices based on this system, particularly for high-frequency[4] and non-linear optical[5] applications.

The organization of the paper is as follows. In Sec. II the experimental details are given and in Sec. III the results obtained for acoustic and optic phonons are presented and discussed. Conclusions are drawn in the final section.

II. EXPERIMENT

Several $InSb/In_{1-x}Al_xSb$ superlattices of various layer thicknesses and compositions were deposited from high-purity targets of InSb, Sb, and Al on (001) InSb substrates in a MSE system.[3,6] Getter purified ultrahigh-purity argon gas was used for the sputter discharge with a typical operating pressure range 1–3 mtorr. This pressure range is sufficient to maintain a highly stable sputter discharge

and yet low enough to ensure that no gas-phase reactions take place (molecular flow regime). The compositions of the ternary layers were determined from double-crystal x-ray diffractometer scans of single-layer test structures and by fitting the x-ray diffractometer scans of the super-lattices.[7] The crystalline quality of the epilayers was evaluated using x-ray diffraction and transmission electron microscopy. The individual layer thicknesses and ternary composition were chosen to ensure that the superlattices did not relax, as evidenced by x-ray line broadening, transmission electron microscopy, and optical phase contrast microscopy. The relevant parameters of the MSE-grown samples, all of excellent epitaxial quality, are summarized in Table I.

The light scattering measurements were carried out using the Brewster-angle quasibackscattering geometry with the angle of incidence set at 70.7° (Brewster's angle for InSb at 647.1 nm). The Raman spectrum was excited with 300 mW of 647.1-nm krypton laser light, frequency analyzed with a Spex 14018 double monochromator, detected with a cooled RCA 31034A photomultiplier, and recorded under computer control. The incident light (directed along X outside the sample) was polarized in the scattering plane and the polarization of the scattered

TABLE I. Physical data for the $InSb/In_{1-x}Al_xSb$ superlattices.

Sample	No. of periods	d (Å)	d_1 (Å)	d_2 (Å)	x
A	20	131.0	58.0	73.0	0.244
B	20	127.6	58.0	69.6	0.186
C	20	125.4	58.0	67.4	0.151
D	20	153.8	70.0	83.8	0.211
E	20	130.5	58.0	72.5	0.217
F	20	137.3	58.0	79.3	0.259
G	20	143.8	58.0	85.8	0.310
H	20	122.0	72.0	50.0	0.364
I	20	116.8	67.0	49.8	0.414
J	20	113.5	72.5	41.0	0.439
K	40	147.5	111.5	36.0	0.161
L	20	122.0	53.6	68.4	0.270

    <u>48</u>   11 228

light (collected at 90° to X along Y outside the sample) was not analyzed. All measurements were carried out at room temperature in a helium-gas atmosphere, which was used to eliminate air features from the spectrum.

III. RESULTS AND DISCUSSION

A. Acoustic phonons

Raman scattering by acoustic phonons is of special interest in semiconductor superlattices. The periodic layering of different materials leads to a new periodicity along the growth direction and to the appearance in the Raman spectra of so-called folded acoustic modes that depend on the superlattice period d, average sound velocity V_{SL}, and refractive index of the materials n_{SL} at the incident laser light wavelength. A number of different approaches have been used to model the acoustic modes in superlattices,[8-10] but Rytov's elastic wave model[8] that has successfully described acoustic phonons in different GaAs/Ga$_{1-x}$Al$_x$As superlattices[11,12] is expected to be appropriate for InSb/In$_{1-x}$Al$_x$Sb superlattices.

In a superlattice made up of alternating layers of thickness d_1 and d_2, the periodicity $d = d_1 + d_2$ leads to a much smaller Brillouin zone (a minizone, with maximum wave vector $q_{max} = \pi/d$) compared to the original Brillouin zone ($q_{max} = 2\pi/a$, where a is the lattice constant). Thus the longitudinal-acoustic branch of the bulk crystal is folded back in the superlattice case, giving many branches which intersect the $q = 0$ axis. For large d (more than approximately ten atomic layers per period) and for frequencies less than ~ 100 cm^{-1} the folded acoustic phonon dispersion may be assumed to be linear and can be described by[12]

$$\omega = V_{SL}[2\pi/d \pm q] , \quad (1)$$

where $m = 0, 1, 2, \ldots$ is the zone folding index and q is the superlattice wave vector. The acoustic velocity in the superlattice is given in Rytov's theory by

$$V_{SL} = d \left[\frac{d_1^2}{V_1^2} + \frac{d_2^2}{V_2^2} + \left(R + \frac{1}{R} \right) \frac{d_1 d_2}{V_1 V_2} \right]^{-1/2} , \quad (2)$$

with $R = \rho_2 V_2 / \rho_1 V_1$, and where V_1 and V_2 and ρ_1 and ρ_2 are the sound velocities and densities for InSb and In$_{1-x}$Al$_x$Sb layers, respectively. The component of the light wave vector perpendicular to the layers in the quasi-backscattering geometry is given by

$$q_p \approx \frac{4\pi n_{SL}(\lambda)}{\lambda} \left[1 - \frac{1}{4[n_{SL}(\lambda)]^2} \right] , \quad (3)$$

where λ is the incident laser light wavelength.

One can see from Eqs. (1), (2), and (3) that the densities ρ_1 and ρ_2, sound velocities V_1 and V_2, and refractive indexes n_1 and n_2 for the InSb and In$_{1-x}$Al$_x$Sb layers, respectively, are needed to calculate the theoretical spectrum using Rytov's model. In the present study, we have used a linear interpolation between pure-InSb and pure-AlSb values taken to be $\rho = 5.775$ g/cm^3, $\rho_{AlSb} = 4.218$ g/cm^3, $V_{InSb} = 3.42 \times 10^5$ cm/s, $V_{AlSb} = 4.53 \times 10^5$ cm/s,

n_{InSb} (647.1 nm) = 4.363, and n_{AlSb} (647.1 nm) = 3.829 (Refs. 13–15) for calculating the alloy ρ_2, n_2, V_2 and superlattice n_{SL}, V_{SL} parameters.

Low-frequency Raman spectra for some of the samples investigated are shown in Fig. 1. At laser light wavelength $\lambda = 647.1$ nm the scattered momentum q_p is less than q_{max} for all samples, i.e., well within the Brillouin zone, and so Eq. (1) applies. Raman spectra for all samples where the acoustic modes were investigated show three or four resolved doublets. The experimental and calculated frequency shifts are given in Table II. The absolute instrumental error in the determination of the experimental frequency shift ω_{exp} is ± 0.4 cm^{-1}. The agreement between the frequencies calculated with Rytov's theory and the observed peak positions is excellent and is within an average accuracy of about 5%. Most of this error probably originates from the linear interpolation used in deducing the density ρ_2 and the sound velocity V_2 of the In$_{1-x}$Al$_x$Sb alloy layer. Another reason for this error may come from the assumption of linear dispersion for the folded phonons, but this is a comparatively small error.

Some additional features were observed for samples H, I, and J. They have frequencies that correspond to scattering from minizone edge (ZE) phonons with $q = q_{max}$. These are also included in Table II and marked ZE. Such ZE acoustic phonon peaks are commonly seen in the Raman spectra of III-V compound superlattices.[1,2]

Table II also contains experimental and calculated intensities of the Raman peaks for the samples. The experimental intensities are given in units of photomultiplier counts/s. The Raman intensities of the folded acoustic phonons were calculated using the formula[12]

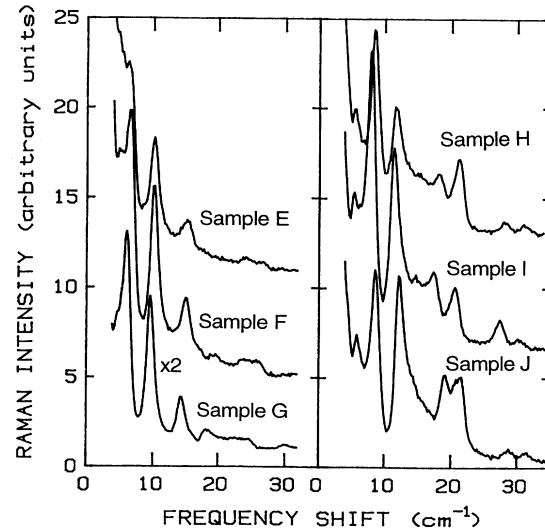$$I \propto m^{-2} \sin^2(m \pi d_1 / d) \omega_m (n_m + 1) \quad (4)$$

FIG. 1. The room-temperature Raman spectra of acoustic phonons in the InSb/In$_{1-x}$Al$_x$Sb superlattices excited with 647.1-nm laser light and recorded in $X(YZ + YX)Y$ polarization with an experimental resolution of 0.8 cm^{-1}. $X(YZ + YX)Y$ polarization corresponds closely to $x(y'y' + y'z')\bar{x}$ polarization within the sample.

TABLE II. Experimental and calculated Raman peak frequencies (ω) and intensities (I) of folded longitudinal acoustic modes in InSb/In$_{1-x}$Al$_x$Sb superlattices. The assignments are given by folding index m or ZE in the case of zone edge peaks.

m	ω_{exp} (cm^{-1})	ω_{calc} (cm^{-1})	I_{exp} (count/s)	I_{calc}	ω_{exp} (cm^{-1})	ω_{calc} (cm^{-1})	I_{exp} (count/s)	I_{calc}	ω_{exp} (cm^{-1})	ω_{calc} (cm^{-1})	I_{exp} (count/s)	I_{calc}
	Sample E				Sample F				Sample G			
0		1.47				1.48				1.47		
-1	$\sim$7	7.1	5590	5090	6.2	6.7	9930	9120	5.9	6.5	17 690	16 100
$+1$	10.1	10.1	4580	5090	9.9	9.7	8320	9120	9.6	9.5	14 520	16 100
-2	15.2	15.7	1350	160	14.8	15.0	2690	530	14.3	14.4	4 400	750
$+2$		18.7		160	19.0	18.0	270	530	18.4	17.4	1 430	750
-3	24.4	24.4	350	430	23.8	23.3	670	600	23.3	22.4	940	380
$+3$	$\sim$27	27.3	280	430	25.4	26.2	690	600		25.4		380
-4		33.0		140		31.5		420	30.1	30.4	530	500
$+4$		36.0		140		34.5		420		33.4		500
	Sample H				Sample I				Sample J			
0		1.47				1.48				1.48		
ZE	5.3	4.9	1060		5.5	4.9	2 280		5.5	5.0	2410	
-1	8.4	8.3	7140	5640	8.0	8.3	12 740	10 920	8.3	8.5	8070	8470
$+1$	11.7	11.4	4150	5640	11.6	11.2	9 100	10 920	12.1	11.5	8870	8470
ZE					14.8	14.6	2 430					
-2	18.0	18.1	2030	440	17.4	18.0	3 190	600	18.9	18.5	4030	1510
$+2$	21.2	21.2	2380	440	20.7	21.0	2 730	600	20.9	21.4	4030	1510
-3	28.1	27.9	530	300	27.5	27.7	1 300	770	28.4	28.5	460	480
$+3$	31.0	31.1	480	300	30.2	30.7	500	770	30.9	31.4	460	480
-4	37.8	37.8	170	310	36.8	37.5	110	450	38.2	38.5	200	630
$+4$	40.7	40.9	210	310	40.3	40.5	80	450	41.3	41.4	230	630

with the $\omega_m(n_m+1)$ Bose factor ignored. The calculated intensities I_{calc} are normalized to the mean experimental intensity of the $m=1$ doublet and rounded to the nearest 10. As seen from Table II, there is no satisfactory agreement between I_{exp} and I_{calc} for $m=2$, although there is reasonable agreement for the $m=3$ case. For samples with approximately equal layer thicknesses, the intensity of even-m peaks should be relatively insignificant [see Eq. (4), when $d_1=d_2=d/2$], but experimentally they are much more intense than the theory predicts. However, it was found for GaSb/AlSb (Ref. 16) and GaAs/Ga$_{1-x}$Al$_x$As (Ref. 12) superlattices that the folded-phonon scattering intensities can be significantly altered under resonant conditions: The even-m phonon intensities can be strongly enhanced. In this study, the large differences in I_{exp} and I_{calc} for the $m=2$ peaks are most likely due to the energy of the exciting light being near an electronic energy gap of one of the superlattice layers (e.g., the E_1 gap in bulk InSb at 300 K is 1.9 eV or 650 nm). The asymmetric line shape of the phonon peaks suggests a coupling between the discrete phonons and a background continuum.

B. Optic phonons

The most widely studied features in all types of superlattices have been the optical phonons, from both the theoretical and experimental points of view.[1,2] The Raman spectrum of superlattices at higher frequencies usually exhibits first-order features characteristic of the two materials comprising the alternating layers. In the case of InSb/In$_{1-x}$Al$_x$Sb superlattices, studies of phonons re-lated to the In$_{1-x}$Al$_x$Sb alloy layers are of considerable interest for their aluminum concentration behavior.

Studies of phonons in mixed crystals have usually revealed a phonon frequency concentration dependence that is classified as either one- or two-mode behavior.[17,18] In the one-mode case, the frequency of the phonon varies continuously with concentration from the frequency characteristic of the one end member to that of the other. In the two-mode case, two phonon peaks are observed in the mixed-crystal spectrum close in frequency to those found for the respective end members. More recently, however, three- and even ten-mode behavior has been observed in mixed crystals.[19-22] One of the most successful methods used to treat two-mode behavior of a mixed crystal is the random element isodisplacement (REI) model proposed by Chen, Shockley, and Pearson[23] and its subsequent modification (MREI model).[24] According to the MREI model, two-mode behavior occurs when $M_{A,C}/M_B>1$, where M_B is the mass of ions B in the mixed crystal with composition ABC and $M_{A,C}$ is the reduced mass given by $M_{A,C}^{-1}=M_A^{-1}+M_C^{-1}$. In our case $M_{In,Sb}/M_{Al}=2.19>1$ and two-mode behavior is expected for In$_{1-x}$Al$_x$Sb optical phonons.

Figure 2(a) shows a typical InSb/In$_{1-x}$Al$_x$Sb superlattice Raman spectrum. The strongest peak at 188 cm^{-1} is due to the longitudinal optical (LO) phonons of the InSb layers, while the less intense peaks near 177 cm^{-1} (InSb-like) and 295 cm^{-1} (AlSb-like) are associated with the two LO phonons predicted in the alloy layers. The weaker structure observed near 100 cm^{-1} and a wide band with a maximum near 335 cm^{-1} are second order in origin.[25] Another sharp peak is seen at 376 cm^{-1}. This is
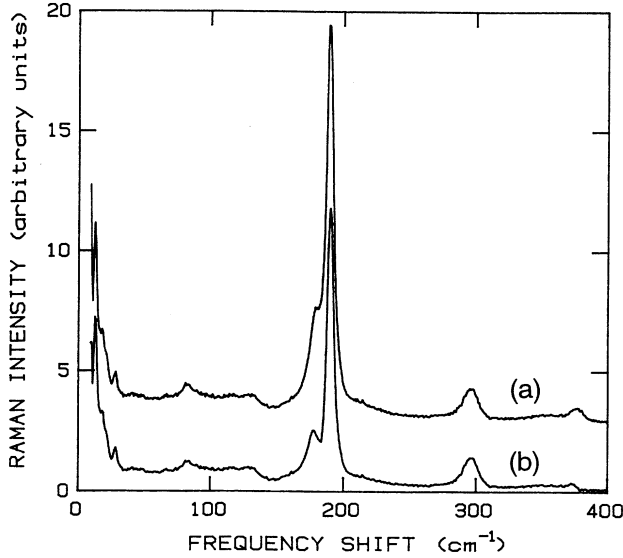
FIG. 2. Room-temperature Raman spectrum of a 20-period InSb/In$_{1-x}$Al$_x$Sb superlattice (sample I) with $x = 0.414$ (a) before and (b) after subtraction of the InSb reference spectrum. The spectral resolution was 2.3 cm^{-1}.

the second-order LO peak in the InSb layer resonantly enhanced, because the exciting light lies close in energy to the E_1 gap in InSb. A reference Raman spectrum of an InSb epilayer was also recorded and used to help reveal the alloy layer spectrum by scaling intensities at the 188 or 376 cm^{-1} line positions and subtracting. The resulting subtracted spectrum (the lines at 376 cm^{-1} were used for scaling in this case) is shown in Fig. 2(b). Although the subtraction process did not entirely remove the 188-cm^{-1} InSb-layer peak, because of a difference between the intensity ratios of the 188- and 376-cm^{-1} lines in the superlattice and InSb-epilayer cases, the lower frequency alloy peak at 177 cm^{-1} is now clearly revealed.

The frequencies of these three LO phonons in the Raman spectra for all superlattices are shown in Fig. 3. It is evident from this figure that all three lines have a linear dependence with aluminum concentration x. A least-squares fit of a straight line to the frequency data for the three lines yielded

$$\omega_{\text{InSb}} = 187.2 + 2.9x \ (\text{cm}^{-1}) \tag{5}$$

for the InSb line,

$$\omega_{\text{InSb-like}} = 186.8 - 23.7x \ (\text{cm}^{-1}) \tag{6}$$

for the InSb-like alloy line, and

$$\omega_{\text{AlSb-like}} = 291.3 + 10.6x \ (\text{cm}^{-1}) \tag{7}$$

for the AlSb-like alloy line. With decreasing x, the InSb-like alloy line increases in frequency and merges eventually with the InSb line at $x = 0$ (within the experimental error), as would be expected. The higher-frequency AlSb-like alloy line lies well below the bulk AlSb LO-phonon frequency of 340 cm^{-1} (Ref. 26) and is less sensitive to x in comparison with the InSb-like line over the concentra-

tion range studied here $(x < 0.5)$. The 187-cm^{-1} InSb line shifts to higher frequency with increasing x and this together with the large difference in the frequency of the AlSb-like line compared with the bulk AlSb frequency is evidence of strain in the superlattice layers due to the difference in the lattice constants of InSb and In$_{1-x}$Al$_x$Sb. The strain is mostly accommodated in the alloy layer, but the slight frequency shift of the InSb line indicates that a small compensating strain appears in the InSb layer. This compensating strain appears because of the large lattice mismatch, which increases with x.

The lattice strain $\varepsilon_\perp$ in the growth direction is related to the in-plane mismatch strain $\varepsilon_\parallel$ by the relationship[27]

$$\varepsilon_\perp = -[2v/(1-v)]\varepsilon_\parallel , \tag{8}$$

where v is Poisson's ratio and $\varepsilon_\parallel = (a_1 - a_2)/a_2$ is due to the lattice mismatch between the In$_{1-x}$Al$_x$Sb (a_2) and InSb (a_1) layers. The strains $\varepsilon_\parallel$ and $\varepsilon_\perp$ are related to the "biaxial" stress X by the elastic compliances S_{11} and S_{12}:[16]

$$\varepsilon_\perp = 2S_{12}X , \tag{9a}$$

$$\varepsilon_\parallel = (S_{11} + S_{12})X . \tag{9b}$$

According to Anastassakis et al.,[28] when a strain is applied along the major axes of the cubic crystal, the triply degenerate optical mode near zero wave vector is split into a singlet with eigenvector parallel to the stress and a doublet with eigenvectors perpendicular to the stress
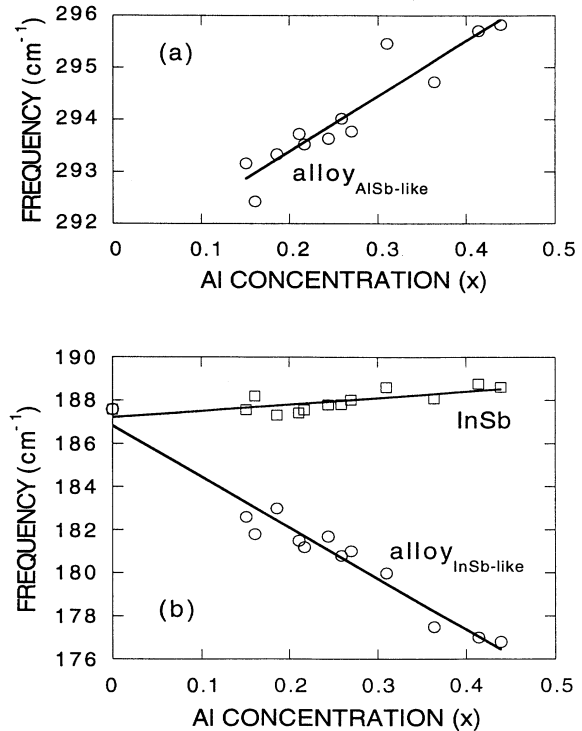

FIG. 3. Concentration dependence of the peak frequencies of (a) the AlSb-like line and (b) the InSb and InSb-like lines in the Raman spectrum of InSb/In$_{1-x}$Al$_x$Sb superlattices at room temperature.

direction. In a backscattering geometry from (001) planes, only the singlet mode is allowed, which corresponds to excitations of vibrations perpendicular to the surface. The shift in the phonon frequency of the singlet mode due to the stress in the $In_{1-x}Al_xSb$ layers of the $InSb/In_{1-x}Al_xSb$ superlattice with $x = 1$ is given by[16,29]

$$\Delta\omega^{LO} = 2\Delta\Omega^H - 2/3\Delta\Omega , \tag{10}$$

where

$$\Delta\Omega^H = \frac{X}{6\omega_0^{LO}}(p + 2q)(S_{11} + 2S_{12}) \tag{11}$$

and

$$\Delta\Omega = \frac{X}{2\omega_0^{LO}}(p - q)(S_{11} - S_{12}) . \tag{12}$$

Here ω_0^{LO} is the unshifted LO frequency in the bulk material. The experimental values $(p - q)/2(\omega_0^{LO})^2 = 0.50$ and $(p + 2q)/6(\omega_0^{LO})^2 = -1.18$, $\omega_0^{LO} = 340$ cm^{-1}, $S_{11} = 1.697 \times 10^{-2}$ GPa^{-1}, and $S_{12} = -0.562 \times 10^{-2}$ GPa^{-1} for AlSb were taken from Refs. 16, 26, and 30. Using Eqs. (9)–(12), we find a tensile stress $X = 4.94$ GPa and frequency shift $\Delta\omega^{LO} = -35.3$ cm^{-1} for AlSb lattice matched to InSb. The stress in the AlSb layer is thus very large, and is comparable to the Ge on Si case, for example, where the compressive stress $X = -6.5$ GPa. The predicted frequency shift is in good agreement with the experimental value of $\Delta\omega^{LO} \approx -38$ cm^{-1} obtained from a linear extrapolation [using Eq. (7)] of the AlSb-like phonon frequency concentration dependence to $x = 1$. Extrapolating Eq. (7) to $x = 0$ allows a prediction for the concentration dependence of the AlSb-like mode in bulk (relaxed) $In_{1-x}Al_xSb$. Assuming a linear relationship between the two end points of 291.3 cm^{-1} (at $x = 0$) and 340 cm^{-1} (at $x = 1$),

$$\omega_{AlSb-like}^{bulk} = 291.3 + 48.7x \ (cm^{-1}) . \tag{13}$$

The optical phonon frequency shift $\Delta\omega^{LO}$ may also be expressed as[31]

$$\Delta\omega^{LO} = -b\varepsilon_\parallel , \tag{14}$$

where b is the strain-shift coefficient relating the displacement of the phonon frequency to the lattice distortion in the plane of growth. Equation (14) may be rewritten in terms of the interfacial biaxial stress X using Eq. (9b) to yield

$$\Delta\omega^{LO} = -b(S_{11} + S_{12})X = -\tau X , \tag{15}$$

where τ is the stress factor, which is different for different phonon lines. An approximate value for the AlSb-like mode stress factor for the $In_{1-x}Al_xSb$ alloy layer can be obtained from Eqs. (14) and (15) by (i) using a linear inter-

polation of the compliances[14,30] S_{11} and S_{12} and lattice constants of pure InSb and AlSb and (ii) using the linear fits to $\omega_{AlSb-like}$ and $\omega_{AlSb-like}^{bulk}$ [Eqs. (7) and (13)] to obtain $\Delta\omega^{LO}$. This yields for τ the expression

$$\tau_{AlSb-like} = 0.17x^2 - 3.8x + 11.3 \ (cm^{-1}/GPa) . \tag{16}$$

Unfortunately, there is no information on the uniaxial strain dependence of the LO mode frequency for bulk InSb (Refs. 32 and 33) and thus the x dependence of the strain in the InSb layers cannot be quantified. For the InSb-like line, a rough estimate for τ can be obtained from the simple assumption that the frequency of this line in the bulk alloy is independent of x to first order. This assumption is justifiable in that the InSb-like line behaves like a gap mode in AlSb, as it lies well below the AlSb line in frequency. (The decrease in bulk alloy lattice constant with increasing x will result in a slight increase of the mode frequency and thus the present estimate forms a lower bound on τ.) With this assumption,

$$\tau_{InSb-like} = 0.11x^2 - 2.4x + 7.1 \ (cm^{-1}/GPa) , \tag{17}$$

which is not too different from the AlSb-like line case [Eq. (16)].

IV. SUMMARY AND CONCLUSION

Strained layer superlattices of $InSb/In_{1-x}Al_xSb$ have been prepared by the technique of magnetron sputter epitaxy. Superlattices with periods of less than 16 nm and alloy compositions $x < 0.5$ have been studied by Raman spectroscopy. The observed frequencies of the zone-folded longitudinal acoustic phonons are in good agreement with calculations based on Rytov's theory of acoustic vibrations in layered media. A photoelastic model for describing the Raman intensities of the folded-phonon doublets is not a good fit to the experimental data in the case where the exciting light energy is near the E_1 gap of the superlattice.

The higher-frequency regions of the Raman spectra consist of the confined LO phonons in the InSb and $In_{1-x}Al_xSb$ layers. The two-mode behavior of the $In_{1-x}Al_xSb$ alloy layer phonons was clearly confirmed. A linear frequency-shift behavior was observed for all LO modes with increasing Al content. Further analysis of the stress-induced changes in the frequencies of the LO modes requires experimental information on the concentration dependence of the mode frequencies in bulk $In_{1-x}Al_xSb$ and on the uniaxial stress dependence of the InSb mode.

ACKNOWLEDGMENT

---

*On leave from the Institute for Low Temperature Physics and Engineering of the Ukrainian Academy of Sciences, Kharkov, Ukraine.

[1] J. Sapriel and B. Djafari Rouhani, Surf. Sci. Rep. **10**, 189

(1989).

[2] B. Jusserand and M. Cardona, in *Light Scattering in Solids V*, edited by M. Cardona and G. Güntherodt, Topics in Applied Physics Vol. 66 (Springer-Verlag, Berlin, 1989), p. 49.

[3]R. Rousina and J. B. Webb, Semicond. Sci. Technol. **6**, C42 (1991).

[4]J. R. Soderstrom, J. Y. Yao, and T. G. Andersson, Appl. Phys. Lett. **58**, 708 (1991).

[5]D. Walrod, S. Y. Auyang, P. A. Wolff, and W. Tsang, Appl. Phys. Lett. **56**, 218 (1990).

[6]J. B. Webb, G. H. Yousefi, and R. Rousina, Appl. Phys. Lett. **60**, 998 (1992).

[7]J. B. Webb, D. J. Lockwood, and D. J. Northcott, Appl. Surf. Sci. **70/71**, 526 (1993).

[8]S. M. Rytov, Akust. Zh. **2**, 71 (1956) [Sov. Phys. Acoust. **2**, 68 (1956)].

[9]A. S. Barker, Jr., J. L. Merz, and A. C. Gossard, Phys. Rev. B **17**, 3181 (1978).

[10]S. Yip and Y. Chang, Phys. Rev. B **30**, 7037 (1984).

[11]C. Colvard, R. Merlin, M. V. Klein, and A. C. Gossard, Phys. Rev. Lett. **45**, 298 (1980).

[12]C. Colvard, T. A. Gant, M. V. Klein, R. Merlin, R. Fischer, H. Morkoç, and A. C. Gossard, Phys. Rev. B **31**, 2080 (1985).

[13]D. F. Edwards and R. H. White, in *Handbook of Optical Constants of Solids II*, edited by E. D. Palik (Academic, New York, 1991), p. 501.

[14]O. Madelung, W. von der Osten, and U. Rössler, in *Numerical Data and Functional Relationships in Science and Technology*, edited by O. Madelung, Landolt-Börnstein, New Series, Group III, Vols. 17 and 22, Pt. a (Springer-Verlag, Berlin, 1987).

[15]We used linear interpolation between the nearest refractive indices in Refs. 13 and 14 to obtain n_{InSb} and n_{AlSb} at the laser wavelength.

[16]P. V. Santos, A. K. Sood, M. Cardona, K. Ploog, Y. Ohmori, and H. Okamoto, Phys. Rev. B **37**, 6381 (1988).

[17]I. F. Chang and S. S. Mitra, Adv. Phys. **20**, 359 (1971).

[18]A. S. Barker, Jr. and A. J. Sievers, Rev. Mod. Phys. **47**, Suppl. 2, 51 (1975).

[19]C. Barta, G. F. Dobrzhanskii, G. M. Zinger, M. F. Limonov, and Yu. F. Markov, Fiz. Tverd. Tela (Leningrad) **24**, 2952 (1982) [Sov. Phys. Solid State **24**, 1672 (1982)].

[20]A. Zwick, G. Landa, M. A. Renucci, R. Carles, and A. Kjekshus, Phys. Rev. B **26**, 5694 (1982).

[21]N. M. Gasanly, A. F. Goncharov, N. M. Melnic, and A. S. Ragimov, Phys. Status Solidi B **120**, 137 (1983).

[22]R. W. G. Syme, D. J. Lockwood, N. L. Rowell, and K. S. Chao, Phys. Rev. B **34**, 8906 (1986).

[23]Y. S. Chen, W. Shockley, and G. L. Pearson, Phys. Rev. **151**, 648 (1966).

[24]I. F. Chang and S. S. Mitra, Phys. Rev. **172**, 924 (1968).

[25]W. Kiefer, W. Richter, and M. Cardona, Phys. Rev. B **12**, 2346 (1975).

[26]S. Ves, K. Strössner, and M. Cardona, Solid State Commun. **57**, 483 (1986).

[27]D. J. Lockwood and J.-M. Baribeau, Phys. Rev. B **45**, 8565 (1992).

[28]E. Anastassakis, A. Pinczuk, E. Burstein, F. H. Pollak, and M. Cardona, Solid State Commun. **8**, 133 (1970).

[29]B. Jusserand, P. Voisin, M. Voos, L. L. Chang, E. E. Mendez, and L. Esaki, Appl. Phys. Lett. **46**, 678 (1985).

[30]E. Anastassakis and M. Cardona, Solid State Commun. **63**, 893 (1987).

[31]F. Cerdeira, A. Pinczuk, J. C. Bean, B. Batlogg, and B. A. Wilson, Appl. Phys. Lett. **45**, 1138 (1984).

[32]We are aware only of a hydrostatic pressure study of the LO-phonon frequency shift in InSb: K. Aoki, E. Anastassakis, and M. Cardona, Phys. Rev. B **30**, 681 (1984).

[33]Z. C. Feng, S. Perkowitz, T. S. Rao, and J. B. Webb, J. Appl. Phys. **68**, 5363 (1990).